JURNAL ILMU KEFARMASIAN INDONESIA
Indonesian Journal of Pharmaceutical Sciences
ISSN p-ISSN 1693-1831 (Print) e-ISSN 2614-6495 (Online) PUBLISHER : Faculty of Pharmacy Universitas Pancasila

In silico exploration of Qur'anic-based natural products as potential anticancer BRAF inhibitors via structure-based virtual screening

Evita Sari[1], Gerry Nugraha[1]*, Deden Mula Saputra[2]

[1]*Department of Pharmacy, Faculty of Health and Technology, Universitas 'Aisyiyah, Palembang, 30961, Indonesia.*
[2]*Department of Ilmu al-Quran dan Tafsir, STIQ Al-Lathifiyyah, Palembang, 30151, Indonesia.*

*Corresponding Author: genugraha@unisa-palembang.ac.id

Received: 20 May 2026 / Accepted: 29 August 2026

ABSTRACT: The BRAF V600E mutation, namely the substitution of valine (non-polar/hydrophobic) with glutamic acid (polar/negative) at position 600, mimics biological phosphorylation and stabilizes the kinase in a permanently active conformation (constitutive activation) promoting uncontrolled melanoma cell proliferation. First-generation synthetic inhibitors, such as vemurafenib and dabrafenib, face challenges of clinical resistance owing to protein dimerization. This study aimed to identify novel BRAF V600E inhibitors through an in silico evaluation of the binding affinity and ADMET safety profile of bioactive compounds from 32 Qur'anic natural product plants, utilizing a structure-based virtual screening of 2,308 compounds (2,301 valid compounds after structural filtration). The target (PDB: 3OG7, empirical crystallography resolution 2.45 Å; R-free: 0.258; R-work: 0.212) was used as the receptor. Molecular docking was performed using AutoDock 4.2 with the Lamarckian Genetic Algorithm (LGA). Validation was carried out through 100 redocking replications with a median RMSD value of 0.377 Å (range 0.31–0.43 Å), well below the validity threshold of 2.0 Å. A total of 1,310 compounds (56.9%) meet the SBVS criteria based on interactions at the Cys532 and Asp594 hotspot residues. The three best candidates from ginger *(Zingiber officinale)*: (1) Diarylheptanoid ketone derivative (-11.37 kcal/mol), (2) Glycosylated gingerol derivative (-10.58 kcal/mol), and (3) Hexahydrocurcumin analog (-10.57 kcal/mol), show the highest binding affinity and met Lipinski's Ro5. Ginger derivatives represent promising lead compounds targeting type IIB kinases, with binding energies reaching -11 kcal/mol. However, prior to clinical trials, molecular optimization is recommended to mitigate the risk of cardiotoxicity (hERG, probability 0.635 in compound 3) and hepatotoxicity (DILI, probability 0.364 in compound 2).

KEYWORDS: ADMET; BRAF inhibitor; cancer; molecular docking; structure-based virtual screening.

▪ INTRODUCTION

Cancer is one of the greatest global health challenges. According to the GLOBOCAN 2022 report, there were 20 million new cancer cases and 9.6 million deaths globally [1]. Among the various types of cancer, melanoma is a major concern due to its close association with genetic mutations in the BRAF Proto-Oncogene. The BRAF V600E mutation involves the substitution of the amino acid valine (non-polar/hydrophobic) with Glutamic Acid (polar, negatively charged) at position 600. It is detected in approximately 40–70% of melanoma cases and is also present in several other malignancies, including thyroid, colorectal, and lung cancers, although at lower frequencies [2]. The presence of the negative charge from Glutamic Acid artificially mimics the biological phosphorylation process, tricking the protein into remaining in a permanently active conformation (constitutive activation).

BRAF inhibitor-based therapies such as vemurafenib and dabrafenib [3] and MEK inhibitors such as trametinib have substantially improved clinical outcomes in the treatment of melanoma and other cancers harboring BRAF mutations [4]. However, the long-term effectiveness of these inhibitors is limited by the emergence of drug resistance through BRAF amplification, NRAS mutations, and the formation of BRAF dimers that cannot be inhibited by first-generation inhibitors [5]. This has prompted the search for new inhibitors that are selective, potent, and capable of overcoming drug resistance. Although secondary metabolites are a recognized source, the specific pharmacopoeia of natural products mentioned in the Qur'an

How to cite this article: Sari E, Nugraha G, Indriani O, Saputra DM. In silico exploration of Qur'anic-based natural products as potential anticancer BRAF inhibitors via structure-based virtual screening. Jurnal Ilmu Kefarmasian Indonesia. 2026. 24(2): 407-421.

https://doi.org/10.35814/jifi.v24i2.2138
ISSN: 2614-6495

remains largely underexplored through modern computational methods, representing a unique niche for identifying novel scaffolds against BRAF V600E.

Natural products are one of the main sources of new bioactive compounds, including plants explicitly mentioned in the Qur'an, such as *Nigella sativa* [6], *Olea europaea* (olive) [7], *Punica granatum* (pomegranate) [8], *Zingiber officinale* (ginger) [9], and honey [10], which have been proven to possess pharmacological activities, including antioxidant, anti-inflammatory, and anticancer properties [2]. Active compounds, such as thymoquinone, oleuropein, hydroxytyrosol, punicalagin, and gingerol, are known to have the potential to modulate oncogenic signaling pathways, including BRAF-driven pathways, making them relevant for the development of molecularly targeted cancer therapies. While traditional knowledge often guides natural product research, the systematic *in silico* exploration of compounds explicitly mentioned in the Qur'an, facilitated by an integrated Qur'anic natural compound database curated by our group, which is made publicly available as an open-source repository [11], represents an underexplored scientific avenue. This approach allows for the high-throughput computational screening of a historically and culturally significant compound library to identify novel BRAF V600E inhibitors, thereby bridging traditional wisdom with modern drug discovery. The use of natural products in drug candidate development through computational approaches, particularly structure-based virtual screening, molecular docking, and ADMET prediction, have become indispensable tools for accelerating natural product-based drug discovery [12].

Advances in computational chemistry, particularly Structure-Based Virtual Screening (SBVS)—which systematically encompasses receptor and ligand preparation, molecular docking, scoring and ranking, hit selection, and ADMET filtering—enable the efficient screening of thousands of compounds against the three-dimensional structure of target proteins [13]. SBVS combines molecular docking with scoring algorithms to prioritize compounds based on predicted binding affinity and binding mode, thereby identifying the best candidate inhibitors prior to experimental testing [14]. This approach has proven to be far more time- and cost-efficient than conventional methods.

Based on this background, this study aimed to identify bioactive compounds from Qur'anic natural products with potential as BRAF V600E inhibitors using the SBVS method, analyze the binding affinity and binding interactions of the best candidate compounds in comparison with existing commercial drugs, and evaluate their pharmacokinetic and toxicity profiles (ADMET) in silico. This study is expected to make a significant contribution by identifying novel, predicted potentially safer, and culturally relevant lead compounds from Qur'anic natural resources, specifically targeting BRAF V600E, thereby expanding the chemical diversity explored for this critical oncology target.

▪ MATERIALS AND METHODS

Materials

A total of 2,308 secondary metabolites retrieved from 32 Qur'anic plant species based on an open-access Qur'anic natural product library repository curated by the authors [10]. The crystal structure of BRAF V600E (PDB ID: 3OG7; resolution 2.45 Å; R-work = 0.212; R-free = 0.258) was retrieved from the Protein Data Bank. This structure displays BRAF in complex with PLX4032. The co-crystallized ligand PLX4032 (a vemurafenib analogue) was used to define the ATP-binding site and validate the docking protocol. Meanwhile, clinically approved BRAF inhibitors, vemurafenib and dabrafenib, were included as reference compounds and obtained from PubChem.

Molecular modeling and docking simulations were primarily executed within the YASARA Structure environment (YASARA Biosciences GmbH, Austria). This included receptor preparation and the execution of molecular docking protocols, which utilized the integrated AutoDock 4.2 Lamarckian Genetic Algorithm (LGA) and AutoDock Vina scoring functions. Bioactive compounds were retrieved from the LOTUS database and sketched using ChemDraw, while their pharmacokinetic and toxicity profiles were evaluated via the ADMETlab 3.0 web server. Post-docking analysis and the visualization of ligand–receptor interactions in 2D and 3D spaces were performed using Discovery Studio Visualizer.

Methods

Receptor correction and preparation

The crystal structure of BRAF V600E (PDB ID: 3OG7) was retrieved from the Protein Data Bank (PDB) and imported into YASARA Structure for receptor preparation. Missing residues were modeled using the terminal loop modeling module in YASARA Structure to add the missing amino acids at three sites: the N-terminal loop (Met432–Asp448), internal loop (Glu545–Ser630), and C-terminal loop (Lys601–Ser614). The corrected receptor was saved in the YASARA Scene format (*. sce). Receptor preparation included the removal of crystallographic water molecules, ions, and heteroatoms; addition of hydrogen atoms; adjustment of protonation states at physiological pH 7.4 [13], and energy minimization using the YASARA2 force field AMBER 14 until the energy gradient converged according to the default YASARA criteria.

Correction of missing residues at the N-terminal loop, internal loop, and C-terminal loop was carried out using the loop modeling facility in YASARA Structure. The algorithm employs a knowledge-based homology approach by searching the Protein Data Bank (PDB) for loop templates that structurally match the anchor residues. Multiple loop conformations were generated and hybridized. The best model was selected based on the lowest conformational energy and optimal packing criteria following energy minimization using the AMBER 14 force field. Finally, the structural validity of the remodeled receptor was quantitatively assessed using YASARA's internal evaluation algorithm, specifically focusing on the overall dihedral energy Z-score and overall model quality Z-score.

Method validation (redocking)

The docking protocol was validated by performing 100 independent redocking simulations of the co-crystallized ligand PLX4032. To ensure absolute reproducibility and eliminate manual placement bias, the simulation cell (grid box) was algorithmically constructed using the YASARA Structure environment. The docking grid was centered on the co-crystallized ligand (PLX4032) and extended 5 Å beyond its outermost atoms, encompassing the ATP-binding pocket while excluding regions reconstructed by loop modeling. Based on this algorithmic generation, the precise spatial anchor for the simulation cell center was established at coordinates X = -15.181, Y = -3.663, and Z = 66.579. This automated approach ensures that the entire ATP pocket is covered consistently across all docking runs. The grid box was deliberately defined to exclude regions of the loop that were computationally reconstructed (N-terminal loop Met432-Asp448, internal loop Glu545-Ser630, and C-terminal loop Lys601-Ser614). The grid box was deliberately defined to exclude regions of the loop that were computationally reconstructed (N-terminal loop Met432–Asp448, internal loop Glu545–Ser630, and C-terminal loop Lys601–Ser614) so that all identified ligand–receptor interactions were fully supported by experimental atomic coordinates and not influenced by artifacts from artificially modeled loop conformations. The receptor was kept rigid according to the lock-and-key principle [14], whereas the ligand was treated as flexible. AutoDock LGA was used as the main method with 100 number of runs. The validity of the method was confirmed if the Root Mean Square Deviation (RMSD) value was ≤ 2.0 Å [15]. AutoDock Vina was additionally employed to evaluate the robustness and consistency of the docking results obtained with AutoDock 4.2.

SBVS

The SBVS process was carried out using an automated screening workflow implemented in YASARA Structure. Of the initial 2.308 compounds, seven compounds were eliminated due to invalid (broken) structures, resulting in a total of 2.301 valid compounds screened. Compounds were selected based on a rigid four-step filtering protocol. First, a binding energy threshold of ≤ -8.0 kcal/mol was established as the primary cutoff. Thermodynamically, this ΔG value corresponds to a sub-micromolar to low-micromolar dissociation constant (K_d), which is widely recognized as a stringent benchmark for identifying potent 'hit' compounds in virtual screening campaigns [12]. Furthermore, this threshold was deliberately set slightly below the binding energies of the established positive controls, vemurafenib and dabrafenib (-9.0 to -10.0 kcal/mol). This initial stringency ensures the retention of novel, diverse chemical scaffolds possessing competitive baseline affinities, which were subsequently subjected to criteria, (2) predicted binding affinity equal to or stronger than that of the co-crystallized ligand PLX4032 or the reference inhibitors (vemurafenib and dabrafenib), (3) crucial hydrogen bond formations with the primary hotspot residues Cys532 (hinge region) and/or Asp594 (DFG motif), and (4) binding-pose RMSD ≤ 2.0 Å relative to PLX4032.

Drug-likeness and ADMET prediction

Drug-likeness was first evaluated using Lipinski's Rule of Five (molecular weight ≤ 500 Da, LogP ≤ 5, hydrogen bond donors ≤ 5, hydrogen bond acceptors ≤ 10), followed by the prediction of pharmacokinetic and toxicity properties. The evaluated ADMET parameters included Human Intestinal Absorption (HIA) to predict oral absorption, CYP450 enzyme inhibition (CYP2C9, CYP2D6, CYP3A4) to assess potential drug–drug interactions, hERG channel inhibition for cardiotoxicity risk, Drug-Induced Liver Injury (DILI) for hepatotoxicity, and the Ames test for mutagenicity. Probability values were interpreted using a three-strata classification system: 0.0–0.3 (low/ideal risk), 0.3–0.7 (potential risk/requires caution and molecular optimization), and >0.7 (high risk/basis for discontinuation of candidate development). A threshold value of < 0.7 was used as the initial inclusion criterion; however, compounds with values in the intermediate range (0.3–0.7) were still identified and reported transparently as areas requiring further optimization. Compounds with parameter values below this threshold were categorized as exhibiting a favorable predicted safety profile for further developmental stages.

Statistical analysis

Descriptive statistical analyses were performed to evaluate the reproducibility and robustness of the molecular docking protocol. The Binding energies and ADMET parameters were summarized using descriptive statistics and presented in comparative tables. For the 100 independent redocking iterations, the distribution of binding energy (kcal/mol) and Root Mean Square Deviation (RMSD, Å) values were analyzed. The central tendency and data dispersion were comprehensively reported using the median, interquartile range (IQR), mean, and standard deviation (SD). Finally, Compounds were prioritized according to predicted binding affinity, followed by evaluation of drug-likeness and ADMET properties. Ligand-protein interactions were visualized using the YASARA-Structure and Discovery Studio Visualizer to characterize the binding mode and identify interactions with catalytically important residues.

▪ RESULTS

Receptor correction and preparation

Initial identification of the BRAF structure (PDB ID: 3OG7) revealed 57 residues, indicating the presence of missing residues at three critical sites, which are marked with turquoise circles in the YASARA-Structure visualization. A complete list of the missing residues is presented in Table 1.

Table 1. List of missing amino acids.

No	Location in structure	Amino acid residue	Initial condition
1	N-terminal loop	Met432, Lys433, Lys434, Gly435, His436, His437, His438, His439, His440, His441, Gly442, Ser443, Arg444, Asp445, Ala446, Ala447, Asp448	*Missing*
2	Loop	Glu545, Thr546, Lys547, Leu597, Ala598, Thr599, Glu600, Lys601, Ser602, Arg603, Trp604, Ser605, Gly606, Ser607, His608, Gln609, Phe610, Glu611, Gln612, Leu613, Ser614, Met627, Gln628, Asp629, Ser630	*Missing*
3	C-terminal loop	Lys601, Ser602, Arg603, Trp604, Ser605, Gly606, Ser607, His608, Gln609, Phe610, Glu611, Gln612, Leu613, Ser614	*Missing*

Missing residues are generally located in flexible-loop regions and are difficult to define by X-ray crystallography. After the correction process using the terminal loop facility in the YASARA-Structure, all missing residues were successfully remodeled.

A comparison of the BRAF receptor structure before and after correction for missing residues and energy minimization is shown in Figures 1 and 2, respectively.

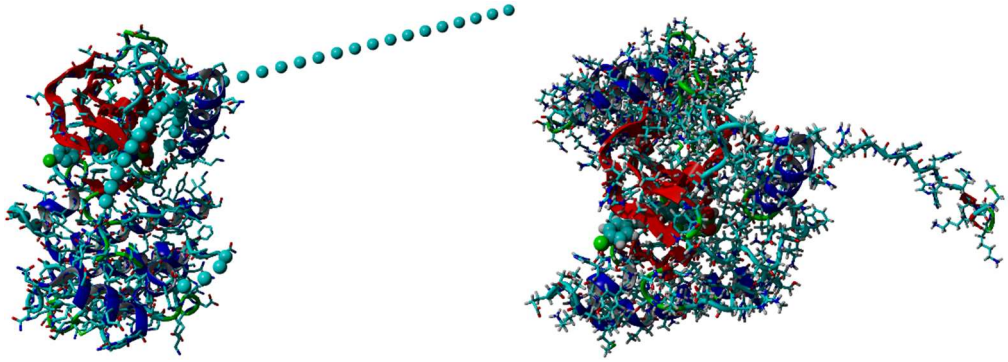

(a) (b)

Figure 1. Visualization of the BRAF V600E receptor (PDB ID: 3OG7): (a) before and (b) after residue correction and energy minimization using the YASARA Structure.

Figure (a) Structure of the BRAF receptor (PDB ID: 3OG7) before correction. The turquoise circles indicate the positions of missing residues in the three loop regions (N-terminal loop, internal loop, and C-terminal loop) that are undefined in the crystallographic data. The presence of these missing residues can affect the accuracy of ligand conformation prediction in the binding pocket if not corrected first. Figure (b) Structure of the BRAF receptor after correction and energy minimization using the YASARA-Structure; all missing residues were remodeled to restore polypeptide chain continuity.

The loop modeling algorithm successfully restored the polypeptide chain continuity of the missing residues. The structural evaluation of the fully remodeled and minimized BRAF receptor yielded an overall dihedral energy Z-score of -1.010 and an overall model quality Z-score of -0.907.

Receptor preparation was followed by placement of the grid box at the ATP-binding pocket, as shown in Figure 2. The yellow-colored receptor indicates a rigid condition (rigid receptor), whereas the grid box defines the ligand search space during the docking process.

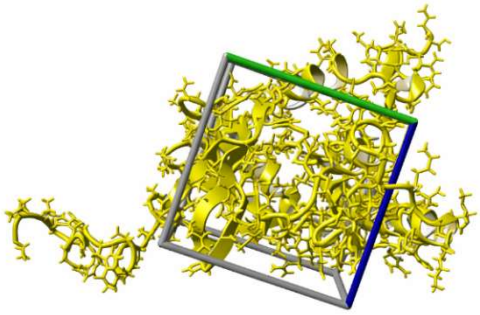

Figure 2. Preparation of BRAF Receptor PDB 3OG7.

Validation of the redocking method

The docking method was validated by redocking the native ligand PLX4032 100 times using two algorithms: AutoDock LGA and AutoDock Vina. The comparison of overlay poses resulting from redocking is shown in Figure 3 (a) and (b).

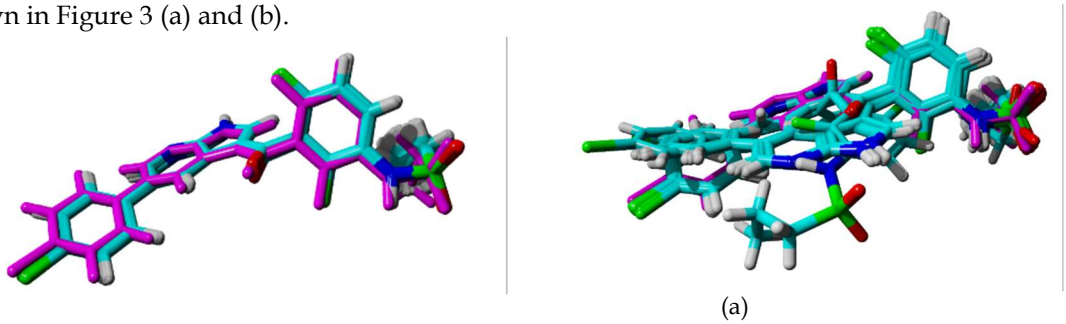

(b) (a)

Figure 3. Visualization of docking results between Autodock LGA and Vina.

Figure (a). Overlay of 100 poses from redocking using AutoDock LGA (magenta = re-docked ligand; cyan = native PLX4032 ligand). All 100 poses stack very consistently at positions nearly identical to the native ligand, reflecting RMSD values of 0.31–0.43 Å (median 0.377 Å). This consistency confirms that LGA accurately reproduces the native ligand-binding position in the ATP pocket of BRAF V600E. **Figure (b)**. Overlay of 100 poses from redocking using AutoDock Vina (magenta = re-docked; cyan = native). Several poses displayed deviations from the native ligand position, as indicated by partial shifts, particularly at the ends of the molecular structure. This variation corresponds to higher and less consistent RMSD values compared to AutoDock LGA, with some runs reaching RMSD > 3.0–5.0 Å, exceeding the validity threshold of ≤ 2.0 Å.

The distribution of binding energy from 100 redocking repetitions using both algorithms is shown in Figure 4 (a) and (b).

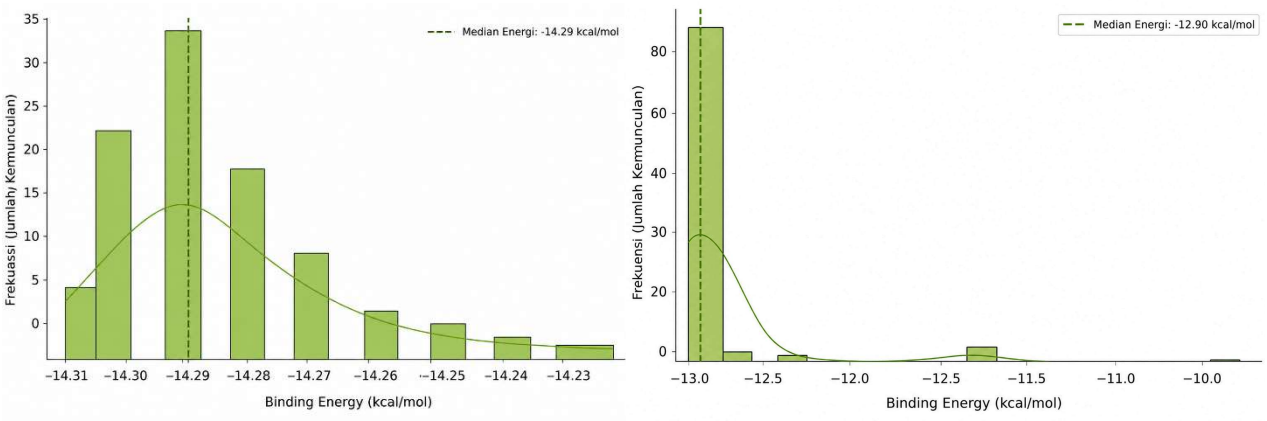

(a) (b)

Figure 4. Comparison of binding energy values between Autodock LGA (a) and Vina (b).

Figure (a). Frequency distribution of binding energy from 100 rounds of redocking using AutoDock LGA. The binding energy values are distributed very narrowly within the range of -14.31 to -14.23 kcal/mol, with a median of -14.29 kcal/mol (dashed line). This distribution, which closely approaches a normal curve with very little variation, demonstrates the high reproducibility of the results and provides a stable algorithm for determining the optimal ligand conformation. Figure (b). Frequency distribution of binding energy from 100 rounds of redocking using AutoDock Vina. The binding energy values are more widely distributed, with a median of -12.90 kcal/mol and a highly left-skewed distribution, where the majority of runs (> 80) yield values around -13.0 kcal/mol, but there are outliers as high as -10.0 kcal/mol. This substantial variation indicates that AutoDock Vina is less consistent in identifying the stable ligand-binding conformations of the BRAF V600E receptor.

The distribution of RMSD values from 100 redocking iterations using both methods is shown in Figure 5 (a) and (b).

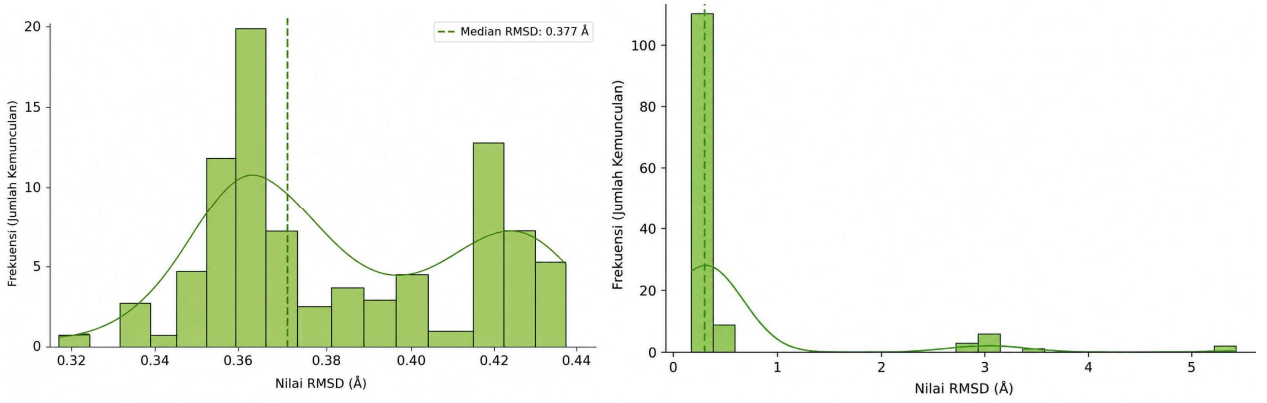

(a) (b)

Figure 5. Comparison of RMSD values between Autodock LGA (a) and Vina (b).

Figure (a). Frequency distribution of RMSD values from 100 redocking runs using AutoDock LGA. All 100 runs (100%) yielded RMSD values within a narrow range of 0.31–0.43 Å with a median of 0.377 Å (dashed line), far below the validity threshold of ≤ 2.0 Å. No single run produced an RMSD > 0.5 Å, confirming that AutoDock LGA consistently and accurately repositions the ligand nearly identically to the native ligand in the protein crystal. These results establish AutoDock LGA as a valid docking protocol for SBVS. **Figure (b)**. Frequency distribution of RMSD values from 100 redocking runs using AutoDock Vina. Although the majority of runs (> 85) produced RMSD < 1.0 Å, there were several runs with significant deviations, with RMSD values reaching 3.0 Å and even > 5.0 Å. This inconsistency indicates that AutoDock Vina occasionally generates ligand poses that do not reflect the original binding position (false-positive conformation); thus, it was not selected as the primary method in this study.

Statistical analysis of the 100 redocking runs using AutoDock LGA demonstrated exceptional reproducibility. The binding energy values exhibited a remarkably narrow distribution with a mean of -14.287±0.015 kcal/mol, a median of -14.290 kcal/mol, and an interquartile range (IQR) of 0.020 kcal/mol. Similarly, the spatial precision was validated by the RMSD distribution, which yielded a mean of 0.387±0.029 Å, a median of 0.377 Å, and an IQR of 0.051 Å. These tight statistical parameters comprehensively validate the stability of the LGA protocol without any structural outliers.

SBVS and ADMET results

A total of 2,308 Qur'anic natural compounds derived from 32 plants mentioned in the Qur'an were screened; seven compounds were eliminated due to invalid (broken) structures, resulting in 2,301 valid compounds moving on to the selection stage. Based on the selection of important amino acid hotspot residues, namely Cys532 (hinge region) and Asp594 (DFG motif) with a binding energy value ≤ -8.0 kcal/mol, a total of 1,310 compounds (56.9%) met the SBVS selection criteria.

The compounds that passed the SBVS selection were then evaluated using ADMETlab 3.0, based on ADMET parameters, which included: (1) Human Intestinal Absorption (HIA), (2) cardiotoxicity via hERG channel inhibition, (3) hepatotoxicity (DILI), (4) mutagenicity (Ames test), (5) CYP2C9 inhibition, (6) CYP2D6 inhibition, and (7) CYP3A4 inhibition. A probability threshold value of ≤ 0.7 was used as the selection criterion, referring to the food therapeutic approach that utilizes natural ingredients without synthetic chemical modification. The distribution of the ADMET selection results is as follows.

- 1310 compounds passed the SBVS selection (binding energy, docking pose, and hotspot interaction)
- 459 compounds met the selected ADMET probability threshold (≤ 0.7)
- 20 top compounds were further analyzed based on a combination of binding energy and ADMET profile

The 20 best compounds with the highest combinations of binding energy values and ADMET profiles are presented in Table 2.

Table 2. List of the 20 best compounds from SBVS and ADMET screening results.

Kode LTS	Binding energy	Interacting residues	Ro5	HIA	hERG	DILI	Ames	CYP2C9	CYP2D6	CYP3A4
LTS0100682	-11.37	LYS 483, CYS 532, ASP 594	0.000	0.000	0.391	0.056	0.140	0.012	0.003	0.510
LTS0088059	-10.58	CYS 532, ASP 594, SER 536	0.000	0.248	0.159	0.364	0.447	0.000	0.001	0.001
LTS0153120	-10.57	CYS 532, ASP 594	0.000	0.008	0.635	0.035	0.085	0.003	0.015	0.095
LTS0244211	-10.53	CYS 532, ASP 594	0.000	0.077	0.441	0.084	0.309	0.005	0.002	0.042
LTS0105696	-10.38	LYS 483, ILE 527, CYS 532, ASP 594	0.000	0.159	0.049	0.656	0.679	0.000	0.073	0.289
LTS0199583	-9.32	CYS 532, ASP 594	0.000	0.001	0.062	0.066	0.102	0.005	0.000	0.030

Kode LTS	Binding energy	Interacting residues	Ro5	HIA	hERG	DILI	Ames	CYP2C9	CYP2D6	CYP3A4
LTS0110897	-9.23	LYS 483, GLN 530, CYS 532, ASP 594	0.000	0.553	0.034	0.672	0.256	0.042	0.000	0.057
LTS0267305	-9.18	THR 529, ASP 594, GLN 530, CYS 532, GLY 534	0.000	0.086	0.102	0.424	0.538	0.002	0.000	0.000
LTS0175767	-9.18	THR 529, ASP 594, GLN 530, CYS 532, GLY 534	0.000	0.127	0.102	0.336	0.577	0.000	0.000	0.047
LTS0117079	-9.16	THR 529, ASP 594, GLN 530, CYS 532, GLY 534	0.000	0.016	0.134	0.223	0.459	0.000	0.000	0.000
LTS0090912	-9.16	THR 529, ASP 594, GLN 530, CYS 532, GLY 534	0.000	0.052	0.143	0.177	0.525	0.000	0.000	0.072
LTS0103909	-9.06	CYS 532, ASP 594	0.000	0.051	0.332	0.052	0.132	0.025	0.144	0.628
LTS0252332	-9.02	CYS 532, ASP 594	0.000	0.061	0.071	0.057	0.196	0.001	0.009	0.386
LTS0079225	-8.89	CYS 532, ASP 594	0.000	0.000	0.040	0.021	0.120	0.000	0.035	0.479
LTS0001322	-8.86	LYS 483, CYS 532, ASP 594	0.000	0.542	0.012	0.336	0.345	0.000	0.000	0.000
LTS0108500	-8.82	GLN 530, CYS 532, ASP 594	0.000	0.329	0.014	0.216	0.253	0.000	0.000	0.000
LTS0268251	-8.78	CYS 532, ASP 594	0.000	0.054	0.092	0.223	0.129	0.530	0.024	0.108
LTS0113744	-8.77	LYS 483, CYS 532, ASP 594	0.000	0.623	0.099	0.077	0.045	0.017	0.000	0.000
LTS0042585	-8.77	LYS 483, CYS 532, ASP 594	0.000	0.033	0.060	0.026	0.169	0.197	0.000	0.013
LTS0211340	-8.59	THR 529, CYS 532, ASN 580, ASP 594	0.000	0.028	0.060	0.655	0.604	0.000	0.000	0.307

Description: BE = Binding Energy (kcal/mol); H-bd = number of hydrogen bonds; Hydrophobic = number of hydrophobic interactions; Distance = interaction distance between ligand and hotspot residue (Å). hERG = probability of hERG channel inhibition (cardiotoxicity); DILI = Drug-Induced Liver Injury (hepatotoxicity); Ames = probability of mutagenicity (Ames test); HIA = Human Intestinal Absorption (probability of low absorption); Lipinski = number of Rule of Five violations (0 = no violations = meets criteria for oral drugs); CYP3A4 = probability of CYP3A4 enzyme inhibition. All probability values were on a 0–1 scale, with values < 0.7.

Based on Table 2, the combination of the highest binding energy values and the best ADMET profiles was visualized in the three selected compound structures as the best BRAF inhibitors using ChemDraw, sourced from the LOTUS database as follows.

Table 3. List of the three best candidate braf ınhibitor structures.

Kode LTS	Structure	Information
LTS0100682 (Q105033489)	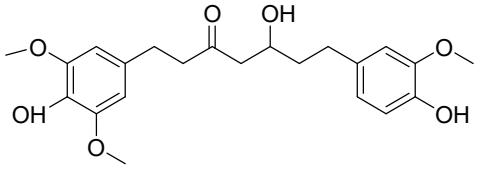	Plant name: Ginger *(Zingiber officinale)* IUPAC name: 5-hydroxy-1-(4-hydroxy-3,5-dimethoxyphenyl)-7-(4-hydroxy-3-methoxyphenyl)heptan-3-one
LTS0088059 (Q105180044)	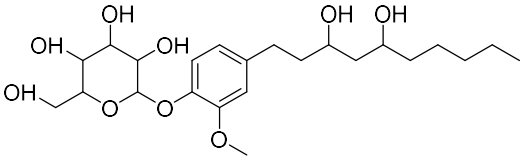	Plant name: Ginger *(Zingiber officinale)* IUPAC Name: (2S,3R,4S,5S,6R)-2-{4-[(3S,5S)-3,5-dihydroxydecyl]-2-methoxyphenoxy}-6-(hydroxymethyl)oxane-3,4,5-triol
LTS0153120 (Q105270970)	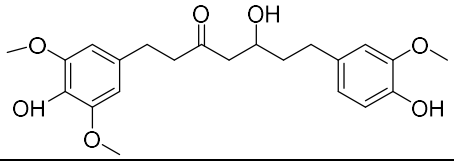	Plant name: Ginger *(Zingiber officinale)* IUPAC name: 1-(4-hydroxy-3,5-dimethoxyphenyl)-7-(4-hydroxy-3-methoxyphenyl)heptane-3,5-diol

Information: All the top candidate compounds were derived from ginger *(Zingiber officinale)*, which is a natural Qur 'anic material. The LTS codes and structures in the table were sourced from the Natural Products Online (LOTUS) database. The 2D structures were visualized using ChemDraw Professional software.

Table 4. Three best BRAF ınhibitor candidates and ıntegrated pharmacokinetic profiles.

Compound identity	BE (kcal/mol)	HIA	hERG	DILI	Ames	CYP3A4	Ro5	Key Interaction	Interpretation
Compound 1: Diarylheptanoid Ketone Derivative (LTS0100682)	-11.37	0.000	0.391	0.056	0.140	0.510	0.000	LYS 483, CYS 532, ASP 594	Low risk; monitor CYP3A4 interactions
Compound 2: Glycosylated Gingerol Derivative (LTS0088059)	-10.58	0.248	0.159	0.364	0.447	0.001	0.000	CYS 532, ASP 594, SER 536	DILI risk (0.364). Further hepatic safety optimization is needed owing to the predicted mutagenicity profile.
Compound 3: Hexahydrocurcumin Analog (LTS0153120)	-10.57	0.008	**0.635**	0.035	0.085	0.095	0.000	CYS 532, ASP 594	Low organ parameter; WARNING: hERG probability 0.635 indicates a potential risk of ventricular arrhythmia, requiring further molecular engineering optimization

Description: The hERG value of 0.635 for compound 3 falls within the intermediate-to-high risk zone (> 0.6), indicating a potential for Ventricular Arrhythmia. Compounds were categorized according to risk strata: 0.0–0.3 = low; 0.3–0.7 = intermediate; and > 0.7 = high.

Analysis showed that compound 3 had an hERG probability of 0.635, indicating a moderate-to-high risk of ventricular arrhythmia. Meanwhile, Compound 2 demonstrated a moderate risk of Drug-Induced Liver Injury (DILI). These data confirm that although the binding energy is very high, modification of the functional

groups is necessary to improve the cardiovascular and hepatic safety profiles before proceeding to the next stage.

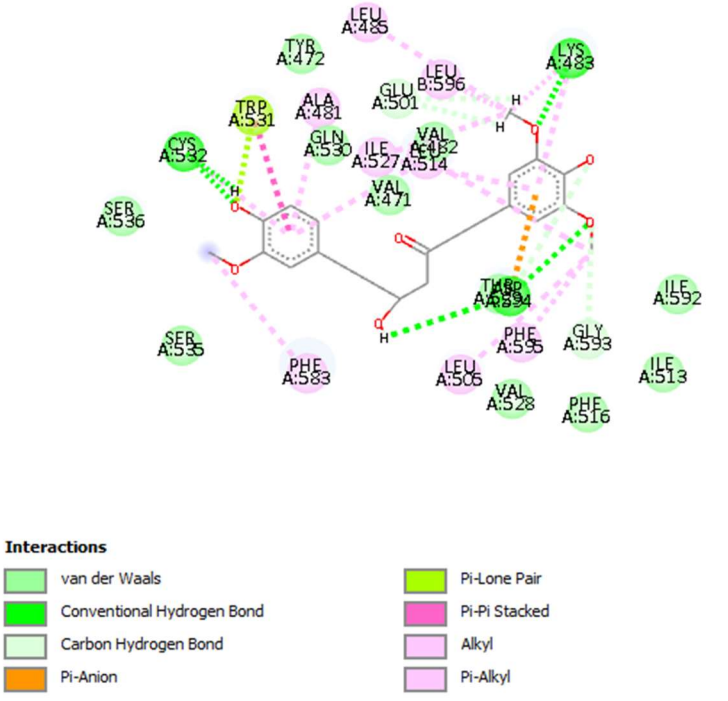

(a)

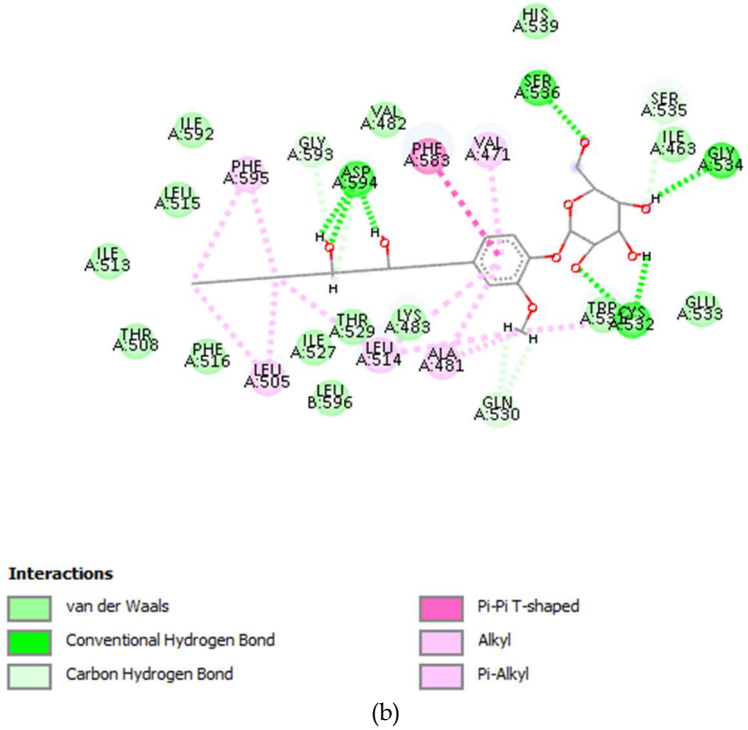

(b)

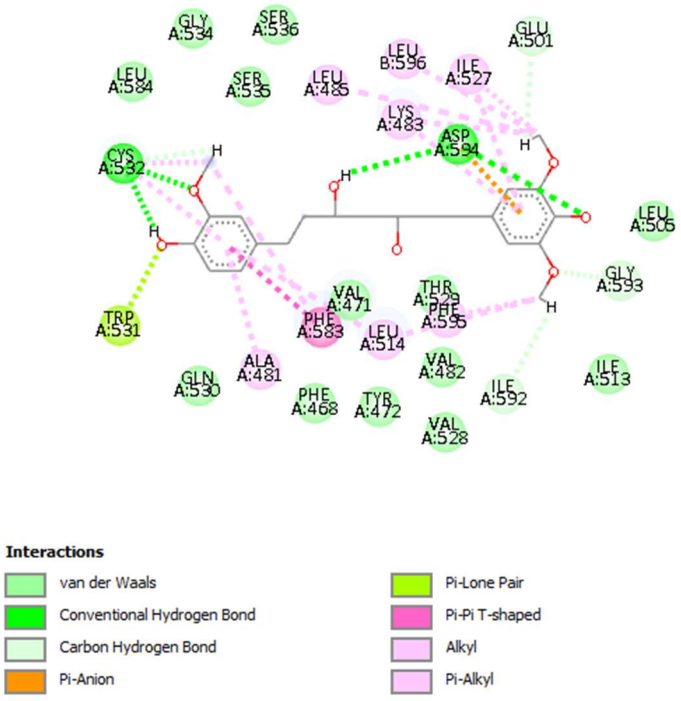

(c)

Figure 6. (a). LTS0100682; (b). LTS0088059; (c). LTS0153120. 2D visualization of the interaction between the ligand and key residues for the three best compounds as candidate BRAF inhibitors was performed using the Discovery Studio Visualizer.

▪ DISCUSSION

This study demonstrated the potential of natural Qur'anic compounds as BRAF V600E inhibitor candidates using a systematic in silico approach encompassing receptor preparation, method validation, SBVS, and ADMET profiling. The findings are discussed in the following sequence. Structure of the BRAF receptor after correction and energy minimization using YASARA-Structure All missing residues were remodeled so that polypeptide chain continuity was restored. Energy minimization with the YASARA2 force field AMBER 14 yielded a stable structure after 1,963 iterations (final energy: -119,929.812 kJ/mol), indicating a thermodynamically optimal conformation ready for docking.

Evaluation of the macromolecular structure quality is crucial prior to molecular docking simulations to ensure that the conformation of the BRAF receptor is geometrically and thermodynamically rational. Based on calculations using the evaluation algorithm in the YASARA Structure software, the BRAF receptor model showed an overall dihedral energy Z-score value of -1.010, representing the quality of the torsion angles (dihedral) of the model structure relative to high-resolution crystallographic structures. Considering that evaluation standards designate a poor quality threshold at values below -2.0, obtaining this value definitively confirms that the backbone geometry and amino acid side chains of the model are excellent and within the range of natural conformations. In addition, the overall model quality Z-score parameter was -0.907, which comprehensively evaluates the three-dimensional structure, including the validity of interatomic interactions and the efficiency of spatial packing. The fact that this value is above the critical threshold further validates that the protein model is free from severe structural errors, such as steric clashes, after the energy minimization cycle. Overall, meeting both of these evaluation parameters provides strong justification that the prepared target receptor structure has a high level of reliability and is highly representative of the subsequent virtual screening stages.

The BRAF receptor after complete preparation, shown in yellow ribbon mode, indicates the rigid receptor conditions used in the docking process. The gray grid box with blue and green accent edges defines the three-dimensional search space encompassing the entire binding site as the docking region.

Method validation for docking was performed by redocking the native PLX4032 ligand in 100 independent replicates using two algorithms: AutoDock LGA and AutoDock Vina. AutoDock LGA produced RMSD values within a narrow range of 0.31–0.43 Å with a median of 0.377 Å (100% of runs below the 2.0 Å validity threshold), far superior to Vina, which generated several runs with RMSD > 3.0–5.0 Å.

From a thermodynamic perspective, LGA simulates natural selection (mutation and coordinate crossover) to navigate ligand conformations in a deep and narrow kinase pocket, thus avoiding energy well traps that may result in false positive conformations. The LGA binding energy distribution was very narrow (-14.31 to -14.23 kcal/mol, median -14.29 kcal/mol), while Vina's was wider with a median of -12.90 kcal/mol. Based on these results, AutoDock LGA was established as the primary docking protocol for the SBVS process [15],[16].

This study successfully identified 1.310 compounds (56.9%) out of 2,301 valid secondary metabolites as candidate BRAF V600E inhibitors through SBVS. The successful validation of the method with a median RMSD value of 0.377 Å (range 0.31–0.43 Å) and 100% run consistency using AutoDock LGA confirms the reliability of the initial docking protocol applied [17],[18]. This is in line with widely accepted docking validation standards, where an RMSD value ≤ 2.0 Å is considered valid and demonstrates the method's ability to reproduce native ligand conformations [19]. AutoDock LGA proved superior in handling the deep and narrow ATP-binding pocket of BRAF, with a very narrow binding energy distribution (-14.31 to -14.23 kcal/mol), indicating high reproducibility and the ability to avoid local energy minima that can produce false-positive conformations.

The main finding of this study is that the three best candidates listed in Tables 3 and 4, namely LTS0100682, LTS0088059, and LTS0153120, are derived from ginger *(Zingiber officinale)* and have more negative binding energy values (-10.57, -10.58, and -11.37 kcal/mol) compared to the positive controls vemurafenib and dabrafenib.(-9.0 to -10.0 kcal/mol) [17],[20]. This indicates the potential for more stable complex formation with BRAF V600E. Dominant interactions at Cys532 (hinge region) and Asp594 (DFG motif) are key characteristics of effective BRAF inhibitors [21],[22]. Binding to Cys532 via hydrogen bonds in the hinge region plays a role in inhibits ATP movement, whereas the interaction with Asp594 in the DFG motif stabilizes the inactive kinase conformation [20].

LTS0100682 is a diarylheptanoid (5-hydroxy-1-(4-hydroxy-3,5-dimethoxyphenyl)-7-(4-hydroxy-3-methoxyphenyl)heptan-3-one) that also interacts with LYS 483, providing the best binding energy of -11.37 kcal/mol. LTS0088059 is a gingerol glycoside that binds to CYS 532, ASP 594, and SER 536, with a binding energy value of -10.58 kcal/mol. LTS0153120 is a hexahydrocurcumin analog (diarylheptanoid) that binds to CYS 532 and ASP 594 with a binding energy of -10.57 kcal/mol. This group of diarylheptanoid compounds aligns with the concept of 'food therapeutics,' as they are derived directly from natural sources. Although this suggests a potentially favorable safety profile compared with synthetic modifications, further experimental validation is essential to confirm both safety and bioavailability.

The three best candidates (LTS0100682, LTS0088059, LTS0153120) are derived from ginger *(Zingiber officinale)* with binding energy values (-10.57 to -11.37 kcal/mol) that are more negative than the positive controls vemurafenib and dabrafenib (-9.0 to -10.0 kcal/mol) [17],[20] indicating the potential formation of a more stable complex with BRAF V600E.

Analysis of the docking mechanism showed that all three compounds formed crucial hydrogen bonds in the hinge region through the Cys532 residue [20]. In addition, the interaction with the Asp594 residue in the DFG motif (aspartate-phenylalanine-glycine) was highly significant. Binding to this DFG motif can lock the BRAF enzyme in its inactive conformation [21],[22], a characteristic that defines these ligands as type IIB kinases. Inhibitors of this type generally display longer residence times and better specificity than type I inhibitors [23]. After establishing the binding affinity, the next critical step was to evaluate the ADMET safety profile in human physiological systems.

Compound 1 (Diarylheptanoid Ketone Derivative) with the best binding energy of -11.37 kcal/mol also interacts with LYS 483, providing an additional anchor outside the ATP pocket. The diarylheptanoid scaffold possesses an elastic aliphatic chain and hydroxyl groups that allow the molecule to slip into narrow hydrophobic pockets while forming stable hydrogen bonds. Compound 2 (Glycosylated Gingerol Derivative) binds to CYS 532, ASP 594, and SER 536, with a binding energy value of -10.58 kcal/mol. Compound 3

(Hexahydrocurcumin Analog) exhibits high selectivity for Cys532 and Asp594 with a binding energy of -10.57 kcal/mol. The phytochemical properties of ginger, including gingerol, shogaol, and zingerone, provide unique structural flexibility for drug design. The diarylheptanoid scaffold features an elastic aliphatic chain and hydroxyl groups that enable this molecule to slip into narrow hydrophobic pockets of the protein. Validation of bioavailability using Lipinski's Rule of Five demonstrated an ideal balance between molecular weight, lipophilicity, and hydrogen bond donor-acceptors for effective oral absorption as a food therapeutic [24], namely, functional compounds that can be obtained directly from natural sources without synthetic chemical modification processes, thus possessing a more natural safety profile and better potential bioavailability.

From a pharmacological safety perspective, hERG evaluation showed varying risk profiles among the three candidates. Compound 1 and Compound 2 have low hERG probabilities (0.391 and 0.159, low-to-moderate risk strata), while Compound 3 shows a hERG probability of 0.635, which falls into the moderate-to-high risk strata, indicating a potential risk of Ventricular Arrhythmia that requires molecular engineering optimization before clinical trials. This assessment follows a three-stratum classification system: 0.0–0.3 (low/ideal risk), 0.3–0.7 (intermediate risk/caution required), and > 0.7 (high risk/stop development). hERG channel inhibition is one of the main causes of drug failure in the clinical stage, as it can cause fatal ventricular arrhythmias [25]. Low DILI values (0.035–0.364) indicated adequate hepatic safety, whereas low Ames values (0.085–0.447) indicated minimal mutagenicity risk. Compliance with Lipinski's Rule of Five (0 violations) for all three compounds indicated good potential oral bioavailability, which is an important prerequisite for anticancer drug development [26]. The use of a 0.7 threshold value in the ADMETlab 3.0 platform, which is a next-generation integrated platform with higher predictive accuracy [27], enables more inclusive yet clinically relevant selection.

From the perspective of Qur'anic natural products, these findings reinforce those of previous studies. Gingerol from ginger *(Zingiber officinale)* inhibits the NF-κB and PI3K/AKT pathways involved in tumor growth [9]. Diarylheptanoid compounds like those identified in this study have also been reported to exhibit antiproliferative activity in various cancer cell lines. This study expands this understanding by demonstrating that secondary metabolites from Qur'anic natural compounds, particularly ginger, possess direct inhibitory potential against BRAF V600E kinase via competitive binding to the ATP pocket. This perspective aligns with QS. Al-An'am [6]: 99, which mentions various beneficial plants as creations for Allah and QS. Al-Insan [76]: 17 regarding a beverage made from ginger, encouraging scientific exploration of the therapeutic potential of plants mentioned in the Qur'an.

The use of ADMETlab 3.0 as an ADMET evaluation platform in this study offers advantages over pkCSM and SwissADME because this platform integrates state-of-the-art machine learning models with a larger and more representative training dataset [27]. The three-strata probability classification system employed 0.0–0.3 (low/ideal risk), 0.3–0.7 (intermediate risk/caution required), and > 0.7 (high risk/stop development), providing a more accurate and transparent interpretive framework than a single-threshold approach. Natural product compounds as food therapeutic products have a long history of empirical use, but this does not eliminate the need for tiered risk assessment to ensure the safety of clinical translation.

This pharmacological analysis confirmed that ginger-derived compounds have significant potential as BRAF V600E inhibitors, with binding energies reaching -11 kcal/mol. However, successful clinical translation is highly dependent on mitigating the risk of cardiovascular and hepatic side effects to moderate levels. This study serves as a logical foundation for resource allocation for further laboratory testing. We acknowledge the LOTUS database for the availability of natural compound data, which is crucial for the integrity of this research [28].

In the context of modern drug discovery, it should be emphasized that several compounds in the polyphenol class have the potential to generate false-positive signals in various screening assays owing to their ability to form nonspecific hydrogen bonds with multiple proteins (promiscuous binding) [21]. Therefore, the computational findings of this study should be interpreted as preliminary hypotheses that require experimental validation. Confirmation through in vitro assays using cancer cell lines harboring the BRAF V600E mutation, particularly selectivity assays against a panel of other kinases to eliminate the possibility of off-target inhibition, as well as assessment of membrane permeability via Caco-2 or PAMPA assays, is unequivocally necessary [29].

CONCLUSION

This study represents one of the first large-scale SBVS investigations of Qur'anic natural products against the BRAF V600E mutation. Three ginger-derived compounds consistently exhibit the strongest binding affinities and are prioritized as lead candidates, suggesting a binding orientation resembling that reported for type IIB kinase inhibitors. Although the docking results demonstrate favorable target binding, ADMET analysis reveals several safety liabilities. Nevertheless, these results provide preliminary computational evidence supporting the pharmacological potential of these compounds. Collectively, these findings establish a computational foundation for the rational development of ginger-derived phytochemicals as potential targeted therapeutics against BRAF V600E-positive cancers. To advance these leads, future investigations must incorporate molecular dynamics simulations and MM/PBSA binding free energy calculations, followed by in vitro kinase assays, selectivity profiling, medicinal chemistry optimization, and ultimately in vivo testing.

Acknowledgements: The author expresses gratitude to the Undergraduate Pharmacy Program, Faculty of Health and Technology, Universitas 'Aisyiyah Palembang for the support of the Computational Chemistry Laboratory facilities, as well as to Dr. Gerry Nugraha, M.Sc., M.Farm. as the first academic advisor and Deden Mula Saputra, S.Th.I., M.Ud as the second academic advisor, who have provided guidance and constructive feedback during the implementation of this research.

Funding: This study did not receive funding from any specific grant-awarding agency in the public, commercial, or non-profit sectors.

Conflict of interest statement: The authors declare no conflicts of interest.

REFERENCES

[1] F. Bray *et al.*, "Global cancer statistics 2022: GLOBOCAN estimates of incidence and mortality worldwide for 36 cancers in 185 countries," *CA. Cancer J. Clin.*, vol. 74, no. 3, pp. 229–263, May 2024, doi: 10.3322/caac.21834.

[2] S. Imani, G. Roozitalab, M. Emadi, A. Moradi, P. Behzadi, and P. Jabbarzadeh Kaboli, "The evolution of BRAF-targeted therapies in melanoma: overcoming hurdles and unleashing novel strategies," *Front. Oncol.*, vol. 14, article 1504142, Nov. 2024, doi: 10.3389/fonc.2024.1504142.

[3] F. A. Dain Md Opo *et al.*, "Identification of novel natural drug candidates against BRAF mutated carcinoma; An integrative in-silico structure-based pharmacophore modeling and virtual screening process," *Front. Chem.*, vol. 10, no. October, pp. 1–21, 2022, doi: 10.3389/fchem.2022.986376.

[4] V. Subbiah *et al.*, "Dabrafenib plus trametinib in BRAFV600E-mutated rare cancers: the phase 2 ROAR trial," *Nat. Med.*, vol. 29, no. 5, pp. 1103–1112, May 2023, doi: 10.1038/s41591-023-02321-8.

[5] Y. Shang *et al.*, "BRAF inhibitor resistance in melanoma: from resistance mechanisms to therapeutic innovations," *Mol. Biomed.*, vol. 7, no. 1, p. 27, Mar. 2026, doi: 10.1186/s43556-026-00425-4.

[6] Y. Ravi *et al.*, "Anticancer potential of thymoquinone from *Nigella sativa* L.: an in-silico and cytotoxicity study," *PLoS One*, vol. 20, no. 6 June, pp. 1–19, 2025, doi: 10.1371/journal.pone.0323804.

[7] S. Jenardhan *et al.*, "Efficacy of olive oil in the reduction of the risk for colorectal cancer – a systematic review," *Int. J. Sci. Res. Biol. Sci.*, vol. 12, no. 1, pp. 27–35, 2025, doi: 10.26438/ijsrbs.v12i1.667.

[8] A. Rauf *et al.*, "The role of pomegranate (*Punica granatum*) in cancer prevention and treatment: modulating signaling pathways from inflammation to metastasis," *Food Sci. Nutr.*, vol. 13, no. 2, e4674, Feb. 2025, doi: 10.1002/fsn3.4674.

[9] M. K. Samota, M. Rawat, M. Kaur, and D. Garg, "Gingerol: extraction methods, health implications, bioavailability and signaling pathways Mahesh," pp. 1652–1669, 2024, doi: 10.1039/d4fb00135d.

[10] A. Kmail, "Honey and cancer : from traditional medicine to modern adjuvant therapy," no. February, pp. 1–18, 2026, doi: 10.3389/fonc.2026.1745285.

[11] Nugraha, G. (2026). Qur'anic-Based Natural Compound Database (Version v1.0.0) [Dataset]. Zenodo. https://doi.org/10.5281/zenodo.22101904. Available at: https://github.com/genugraha/QuranicMolecularDatabase

[12] S. Nafisa, S. U. Noor, A. Azkannufuus, and Y. Noviani, "*Cosmos caudatus* Kunth. leaf extract herbal nanosuspension

formulations, characterization, and cytotoxicity approach against MCF-7 breast cancer cells," *J. Ilmu Kefarmasian Indones.*, vol. 21, no. 2, p. 286, 2023, doi: 10.35814/jifi.v21i2.1481.

[13] A. Altharawi and S. M. Alqahtani, "Integrative computational chemistry approaches in modern drug discovery: advances in docking, pharmacophore modeling, molecular dynamics, and virtual screening," *Pharmaceutics*, vol. 18, no. 5, p. 565, May 2026, doi: 10.3390/pharmaceutics18050565.

[14] E. H. B. Maia, L. C. Assis, T. A. de Oliveira, A. M. da Silva, and A. G. Taranto, "Structure-based virtual screening: from classical to artificial ıntelligence," *Front. Chem.*, vol. 8, no. 343, April, 2020, doi: 10.3389/fchem.2020.00343.

[15] G. Nugraha and E. P. Istyastono, "Virtual target construction for structure-based screening in the discovery of histamine h2 receptor ligands," *Int. J. Appl. Pharm.*, vol. 13, no. 3, pp. 1–3, 2021, doi: 10.22159/ijap.2021v13i3.41202.

[16] Y. S. Kurniawan *et al.*, "Molecular docking and molecular dynamic ınvestigations of xanthone-chalcone derivatives against epidermal growth factor receptor for preliminary discovery of novel anticancer agent," *Indones. J. Chem.*, vol. 24, no. 1, pp. 250–266, 2024, doi: 10.22146/ijc.88449.

[17] B. Wu *et al.*, "Novel natural inhibitors targeting B-RAF(V600E) by computational study," *Bioengineered*, vol. 12, no. 1, pp. 2970–2983, Jan. 2021, doi: 10.1080/21655979.2021.1943113.

[18] J. Carlsson and A. Luttens, "Structure-based virtual screening of vast chemical space as a starting point for drug discovery," *Curr. Opin. Struct. Biol.*, vol. 87, p. 102829, Aug. 2024, doi: 10.1016/j.sbi.2024.102829.

[19] G. Simanullang, A. M. Rahayyu, N. A. Nabila, A. Hammami, and I. K. Wardani, "Molecular docking and pharmacokinetic prediction of isoniazid and curcumin compounds against N-acetyltransferase 2 (NAT2) protein," *J. Ilmu Kefarmasian Indones.*, vol. 23, no. 2, p. 305, 2025, doi: 10.35814/jifi.v23i2.1699.

[20] A. B. Umar and A. Uzairu, "Virtual screening, pharmacokinetic, and DFT studies of anticancer compounds as potential V600E-BRAF kinase inhibitors," *J. Taibah Univ. Med. Sci.*, vol. 18, no. 5, pp. 933–946, 2023, doi: 10.1016/j.jtumed.2023.01.013.

[21] E. Madej *et al.*, "Vemurafenib and dabrafenib downregulates RIPK4 level," *Cancers (Basel).*, vol. 15, no. 3, p. 918, Feb. 2023, doi: 10.3390/cancers15030918.

[22] T. Żołek, A. Mazurek, and I. P. Grudzinski, "In silico studies of novel vemurafenib derivatives as BRAF kinase inhibitors," *Molecules*, vol. 28, no. 13, p. 5273, Jul. 2023, doi: 10.3390/molecules28135273.

[23] A. K. Singh *et al.*, "Challenges and Opportunities in the Crusade of BRAF Inhibitors: From 2002 to 2022," *ACS Omega*, vol. 8, no. 31, pp. 27819–27844, Aug. 2023, doi: 10.1021/acsomega.3c00332.

[24] C. A. Lipinski, F. Lombardo, B. W. Dominy, and P. J. Feeney, "Experimental and computational approaches to estimate solubility and permeability in drug discovery and development settings 1PII of original article: S0169-409X(96)00423-1," *Adv. Drug Deliv. Rev.*, vol. 46, no. 1–3, pp. 3–26, Mar. 2001, doi: 10.1016/S0169-409X(00)00129-0.

[25] J. I. Vandenberg, M. D. Perry, M. J. Perrin, S. A. Mann, Y. Ke, and A. P. Hill, "hERG K(+) channels: structure, function, and clinical significance.," *Physiol. Rev.*, vol. 92, no. 3, pp. 1393–1478, 2012, doi: 10.1152/physrev.00036.2011.

[26] J. Zhang *et al.*, "Computational toxicology in drug discovery: applications of artificial intelligence in ADMET and toxicity prediction," *Brief. Bioinform.*, vol. 26, no. 5, 2025, doi: 10.1093/bib/bbaf533.

[27] L. Fu *et al.*, "ADMETlab 3.0: an updated comprehensive online ADMET prediction platform enhanced with broader coverage, improved performance, API functionality and decision support," *Nucleic Acids Res.*, vol. 52, no. W1, pp. W422–W431, Jul. 2024, doi: 10.1093/nar/gkae236.

[28] A. Rutz *et al.*, "The LOTUS initiative for open knowledge management in natural products research," *Elife*, vol. 11, pp. 1–41, May 2022, doi: 10.7554/eLife.70780.

[29] J. B. Baell and G. A. Holloway, "New substructure filters for removal of pan assay interference compounds (PAINS) from screening libraries and for their exclusion in bioassays," *J. Med. Chem.*, vol. 53, no. 7, pp. 2719–2740, 2010, doi: 10.1021/jm901137j.